Dynamic properties of InAs/InP(311B) quantum dot Fabry-Perot lasers emitting at 1.52-μm

Anthony Martinez, Kamel Merghem, Sophie Bouchoule, Gautier Moreau, Abderrahim Ramdane, Jean-Guy Provost, Francois Alexandre, Frédéric Grillot, Olivier Dehaese, Rozenn Piron, et al.

Dynamic properties of InAs/InP (311)B Quantum Dot Fabry-Perot lasers emitting at 1.52 µm

A. Martinez, K. Merghem, S. Bouchoule, G. Moreau and A. Ramdane
[1] *CNRS Laboratory for Photonics and Nanostructures, Route de Nozay, 91460 Marcoussis, FRANCE*

J.-G. Provost, F. Alexandre
[2] *Alcatel-Thales III-V Lab, Route de Nozay, 91460 Marcoussis, France*

F. Grillot, O. Dehaese, R. Piron, S. Loualiche
[3] *FOTON-INSA Rennes 20 avenue des Buttes de Coesmes, 35043 Rennes Cedex, France*

Abstract: Dynamic properties of truly three dimensional-confined InAs/InP quantum dot (QD) lasers obtained by molecular beam epitaxy (MBE) growth on a (311)B oriented substrate are reported. Relative intensity noise and small signal modulation bandwidth experiments evidence maximum relaxation frequency of 3.9 GHz with a clear relaxation oscillation peak, indicating less damping than InAs/GaAs QD lasers. The Henry factor amounts to ~ 1.8 below threshold and increases to ~ 6 above threshold, which is attributed to band filling of the thick wetting layer.

Quantum-dot (QD) based lasers have raised a lot of interest over the last decade since the early theoretical predictions of unique properties arising from 3-dimensional carrier confinement[1]. Intense research in the growth of self-assembled QDs in the Stranski-Krastanov regime has hence allowed studies of these atomic-like nanostructures. Potential applications in fiber telecommunication pushed forward the development of long wavelength QD lasers both at 1.3 µm on GaAs substrate and on InP substrate for 1.55 µm applications. Indeed, low cost uncooled and isolator-free directly modulated lasers are very attractive for local area and metropolitan area networks. Subsequently, much effort has been devoted to the development of InAs/GaAs QDs with the demonstration of superior performances compared to that of QW based lasers. Unprecedented properties like ultra low threshold current[2], high characteristic temperature[3], increased tolerance to optical feedback[4] have readily been demonstrated. For long-haul applications, lasers emitting at 1.55 µm are desirable as the emission wavelength correspond to the lowest attenuation of silica based optical fibers and to the amplification band of erbium doped fiber optical amplifiers. However, the optical fiber chromatic dispersion induces penalty for data transmission at 1.55 µm. One unique theoretical property of QD lasers relates to the near zero Henry factor at the gain peak of the laser[5]. This is a fundamental characteristic as it should open the way for chirp-less penalty free high bit rate data transmission. Growth using molecular beam epitaxy (MBE) on (100) InP generally leads to elongated dots or so-called Quantum Dashes[6-8]. However, these quasi-1 D nanostructures exhibit a linewidth enhancement factor (LEF) which amounts to ~ 4-6[8,9], similar to that of the best QW lasers. More recently, MBE growth[10] and metal-organic chemical vapour phase epitaxy (MOVPE) [11,12] have allowed the growth of truly three-dimensionally confined QDs on InP (100). No investigation of the LEF has ever been reported in this material system.

An alternative approach, which relies on MBE growth on a specific InP (311)B orientation, has also allowed the formation of QDs with a high dot density of 10^{11} cm^{-2} [13,14]. A very low chirp of 0.01 nm was measured but no direct measurement of the Henry factor was reported[13].

In this paper, we report on the microwave frequency properties – relaxation frequency and Henry factor- of narrow ridge single mode waveguide Fabry-Perot (FP) lasers processed from a 5 InAs/InP (311)B QD layer structure emitting on the ground state (GS) at 1.52 μm. In particular, the Henry factor amounts to ~ 1.8 below threshold while it increases up to ~ 6 just above threshold, which is attributed to band filling of the thick wetting layer.

The laser heterostructure has been grown by molecular beam epitaxy on a (311)B n+-oriented InP substrate. The active region consists of 5 QD layers as described in Ref. 15. A modal gain of 16 cm^{-1} and internal loss of 10 cm^{-1} have been extracted from this layer structure[15]. 3 μm-wide ridge waveguide (RWG) FP lasers were processed by a Cl_2-H_2 induced coupled plasma etching process[16]. Benzocyclobutene (BCB) allows planarization of electrodes with a small parasitic capacitance compatible with 10 Gb/s operation. The investigated lasers have as-cleaved facets. Lasing is observed on the QD ground state (GS) at 1.52 μm at room temperature in continuous wave (CW) for cavities as short as 1030 μm. When the temperature increases from 20°C to 70°C, the threshold current of a 1100 μm-long FP laser increases from 41 mA to 117 mA and the slope efficiency decreases from 0.12 to 0.06 W/A per facet (Fig.1.). Output power in excess of 22 mW is obtained at room temperature, much higher than earlier reports[13,14]. A characteristic temperature of 49 K is extracted, comparable to that observed in InAs/InP QD lasers grown by MOVPE[12]. This is attributed to non radiative Auger recombination that was measured to account for 90% of the total current at room temperature on a similar layer structure[17]. Emission on the QD ground state in CW regime is observed up to 75 °C at 200 mA, indicating the absence of excited state (ES) contribution.

The LEF was then assessed at room temperature below and above threshold on the same device. The Henry factor is defined as - $4\pi/\lambda\times(\delta n/\delta N)/(\delta g/\delta N)$ and represents the variation of the real part of the refractive index change over the differential gain when the carrier density changes. The linewidth enhancement factor was primarily assessed below threshold. Fig.2. depicts the measured net gain when the current is increased from 26 to 41 mA in steps of 3 mA. A net gain of 10 cm^{-1} is obtained at the gain peak of ~ 1522 nm. The Henry factor α_H decreases with the current and amounts to 1.8 at the gain peak just below threshold (Fig.3). As the differential gain decreases near threshold (Fig. 2.), the decrease of the LEF is attributed to an almost vanishing refractive index change. The 'material' LEF of InAs/InP (311)B QD lasers is smaller than that of earlier values of InAs/InP (100) quantum dash (QDash) lasers[8,9], which is attributed to a smaller differential refractive index. We also performed measurement of the differential index and gain within the homogeneous linewidth of the QD population. A similar trend and comparable values are observed at 1517 and 1527 nm, although the α_H at the longer wavelength equals ~ 3.1 due to a lower differential gain.

The evaluation of the 'device' LEF above threshold is more relevant for telecom applications as it corresponds to a regime where sufficient optical power is available for data transmission. To determine the LEF, a high frequency current modulation technique was applied with a modulation frequency of 7 GHz[18]. The LEF is measured at the gain peak and it amounts to 6.8 at ~ 1522 nm just above threshold. A drastic increase of the LEF is indeed evidenced when the laser is biased above threshold. This behaviour is attributed to a plasma effect, similar to that invoked in

InAs/GaAs QDs[19]. We believe that above threshold, the dot GS occupation probability is saturated[19]. This results in a significant band filling of the higher energy levels, i.e. the wetting layer (high degeneracy states) and the barrier/waveguide, that breaks the Gaussian-like symmetry of the gain spectrum. The Henry factor does not noticeably change with the bias current as it amounts to 7.7 at 137 mA. This behaviour is comparable to what was earlier reported in QDash-in-a-well lasers[8]. Reduced non linear gain compression and the absence of ES emission at high injection current in InAs/InP (311)B QD lasers result in a smaller rate of decrease of the differential gain with the current density compared to 5-InAs/GaAs QD layer structures[18]. This explains why no divergence of the Henry factor is observed at high injection current, unlike InAs/GaAs QD lasers where it was attributed to incomplete gain clamping of the ES at the GS threshold gain[20]. The LEF was also measured on two other longitudinal modes at 1517 and 1527 nm (i.e. within the corresponding homogeneous linewidth): similar values of the LEF ~ 7 are obtained just above threshold and the LEF does not exhibit any significant dependence with the carrier density up to $2.5\times i_{th}$. The LEF is thus constant over 10 nm within the homogeneous broadening of the QD ensemble population. Indeed, the high density of final states of the thick wetting layer favours the electron transition back to the wetting layer, which adversely affects the LEF.

Microwave frequency properties were investigated by means of relative intensity noise (RIN) measurements to extract the intrinsic properties of QD lasers. Fig. 4 illustrates the evolution of the relaxation frequency versus the normalized current. The modulation efficiency equals 0.38 GHz/mA$^{1/2}$, lower than 0.63 GHz/mA$^{1/2}$ measured in standard 5 InAs/GaAs QD lasers[18]. The relaxation frequency f_r and the -3 dB bandwidth reach a maximum value of 3.8 GHz and 4.8 GHz respectively at a 137 mA bias current. The evolution of the damping factor against the squared relaxation frequency leads to a K-factor of 0.63 ns, implying a maximum intrinsic modulation bandwidth of 14.1 GHz. The gain compression is accountable for the lower experimental bandwidth, as evidenced in InAs/GaAs QD lasers[21]. Stacking more QD layers into the active region should result in higher modal gain, allowing laser emission from shorter cavities compatible with 10 Gb/s direct modulation. As the K-factor is about 2 times lower than that of standard InAs/GaAs QD layer structures[21], the carrier dynamics in the conduction band of InAs/InP QDs may be governed by a different relaxation process. Small signal modulation bandwidth experiments were subsequently performed using a lightwave component analyzer. Extraction of the relaxation frequency versus the bias current shows nearly identical values to those obtained from RIN measurements, demonstrating a modulation efficiency of 0.36 $GHz/mA^{1/2}$ and a maximum f_r of 3.7 GHz. Taking into account a photon lifetime of 5.8 ps, a differential gain of 7.3×10^{-15} cm^2 is deduced. The evolution of the damping rate versus the current also allows the extraction of the non linear gain coefficient which equals 6.4×10^{-16} cm^3, lower than that of InAs/GaAs QDs lasers, where strong damping was attributed to carrier relaxation from the ES to the GS (so-called phonon relaxation bottleneck[20]). Surprisingly, the peak of the relaxation oscillation is clearly distinguishable in the modulation transfer function of the InAs/InP (311)B QD lasers (inset Fig.4). However, previous work evidenced suppression of relaxation oscillation peak in InAs/InP (311)B QD directly modulated lasers emitting at 1.64 µm[13]. This was attributed to spectral hole burning of isolated dots and we believe that the higher bandgap discontinuity in the conduction band (QD potential) was higher than that of our present device. Therefore, it is conjectured that no such carrier dynamics exist in InAs/InP (311)B QD lasers emitting on the ground state at 1.52 µm as the energy transition between the wetting layer and the QD GS amounts to ~ 100 meV[17], compared to ~ 300 meV for InAs/GaAs QDs emitting at 1.3 μm.

In conclusion, we thoroughly investigated the static and dynamic properties of InAs/InP (311)B quantum dot lasers emitting on the ground state at 1.52 μm. The Henry factor is found to be as low as 1.8 at the gain peak just below threshold and increases to about 6.6 above threshold but remains constant with the current. The rather high value is attributed to band filling of the thick wetting layer (high degeneracy states). The sole emission from the ground state at high current and at a high temperature of 75°C as well as a distinct relaxation oscillation peak in the frequency modulation response indicate the absence of phonon relaxation bottleneck originating from an excited state.

This work has been supported by the EU EPIXnet Network of Excellence.

[1] A. Arakawa and H. Sakaki, Appl. Phys. Lett., 40, 939 (1982)

[2] G. T. Liu, A. Stintz, H. Li, K. J. Malloy, and L. F. Lester, IEE Electron. Lett., 35,1163 (1999)

[3] O.B. Shchekin and D. G. Deppe, IEEE Photon. Technol. Lett., 14, 1231 (2002)

[4] H. Su, L. Zhang, A. L. Gray, R. Wang, T. C. Newell, K. Malloy, and L. F. Lester, IEEE Photon. Technol. Lett. 15, 1504-1506 (2003).

[5] D. Bimberg, N. Kirstaedter, N. N. Ledentsov, Zh. I. Alferov, P. S. Kop'ev, V. M. Ustinov, IEEE J. Sel. Top. Quantum Electron. 3, 196-205 (1997).

[6] R. H. Wang, A. Stintz, P. M. Varangis, T. C. Newell, H. Li, K. J. Malloy, and L. F. Lester, IEEE Photon. Technol. 13, 767-769, (2001).

[7] R. Schwertberger, D. Gold, J. P. Reithmaier, and A. Forchel, "Long-wavelength InP-based quantum-dash lasers," IEEE Photon. Technol. 14, 735-737 (2002).

[8] F.Lelarge, B. Dagens, J. Renaudier, R. Brenot, A. Accard, F. van Dijk, D. Make, O. Le Gouezigou, J.-G. Provost, F. Poingt, J. Landreau, O. Drisse, E. Derouin, B. Rousseau, F.Pommereau, and G.-H. Duan, IEEE J. of Selec. Topics in Quant. Electron., Vol. 13, N° 1, 111 (2007)

[9] A. A. Ukhanov, R. H. Wang, T. J. Rotter, A. Stintz, L. F. Lester, P. G. Eliseev, and K. J. Malloy, Appl. Phys. Lett. 81, 981 (2002).

[10] J. S. Kim, J. H. Lee, S. U. Hong, W. S. Han, H. Kwack, C. W. Lee, D. K. Oh, IEEE Photon. Technol. Letters, 16, 7, 1607 (2004)

[11] D. Franke, M. Moehrle, J. Boettcher, P. Harde, A. Sigmund, and H. Kuenzel, Appl. Phys. Lett., 91, 081117 (2007)

[12] S. Anantathanasarn, R. Nötzel, P. J. van Veldhoven, F. W. M. van Otten, Y. Barbarin, G. Servanton, T. de Vries, E. Smalbrugge, E. J. Geluk, T. J. Eijkemans, E.

A. J. M. Bente, Y. S. Oei, M. K. Smit, and J. H. Wolter, Appl. Phys. Lett., 89, 073115, (2006)

[13] H. Saito, K. Nishi and S. Sugou, IEE Electron. Lett., Vol. 37 No. 21, Oct. 2001

[14] P. Caroff, C. Paranthoen, C. Platz, O. Dehaese, H. Folliot, N. Bertru, C. Labbé, R. Piron, E. Homeyer, A. Le Corre, and S. Loualiche, Appl. Phys. Lett., 87, 243107 (2005)

[15]G. Moreau, K. Merghem, A. Martinez, S. Bouchoule, A. Ramdane, F. Grillot, R. Piron, O. Dehease, E. Homeyer, K. Tavernier, S. Loualiche, P. Berdaguer and F. Pommerau, IET Optoelectron., 1, (6), 255–258 (2007).

[16] S. Guilet, S. Bouchoule, C. Jany, C. S. Corr, and P. Chabert, J. Vac. Sci. Technol. B, vol.24(5), 2381 – 2387 (2006).

[17] N. F. Massé, E. Homeyer, I. P. Marko, A. R. Adams, and S. J. Sweeneya, O. Dehaese, R. Piron, F. Grillot, and S. Loualiche, Appl. Phys. Lett., 91, 131113 (2007)

[18]D.-Y. Cong, A. Martinez, K. Merghem, G. Moreau, A. Lemaître, J.-G. Provost, O. Le Gouezigou, M. Fischer, I. Krestnikov, A.R. Kovsh, and A. Ramdane, IEE Electron. Lett. 43, 222 (2007)

[19]S. Melnik, G. Huyet, and A. Uskov, Optics Express, 14, 2950 (2006)

[20]A. Markus, J. X. Chen, O. Gauthier-Lafaye, J.-G. Provost, C. Paranthoën, and A. Fiore, IEEE J. Sel. Top. Quantum Electron., 9, 1308 (2003)

[21] H. Su, and L. F. Lester, J. Phys., D: Appl. Phys. **38**, 2112 (2005)

Figure Captions:

FIG. 1. L-I characteristics of a 1100 µm-long Fabry-Perot laser with as-cleaved facets for temperature from 20 to 80°C in CW regime and characteristic temperature (inset).

FIG. 2. Net gain at 20°C in CW regime of a 1100 µm-long Fabry-Perot laser versus current below threshold.

FIG. 3. Henry factor below and above threshold of a 1100 µm-long InAs/InP (311)B QD Fabry-Perot laser.

FIG. 4. Relaxation frequency measured from the RIN and small signal modulation bandwidth experiments versus the normalized current at 20°C (inset: transfer function at 50 and 77 mA).

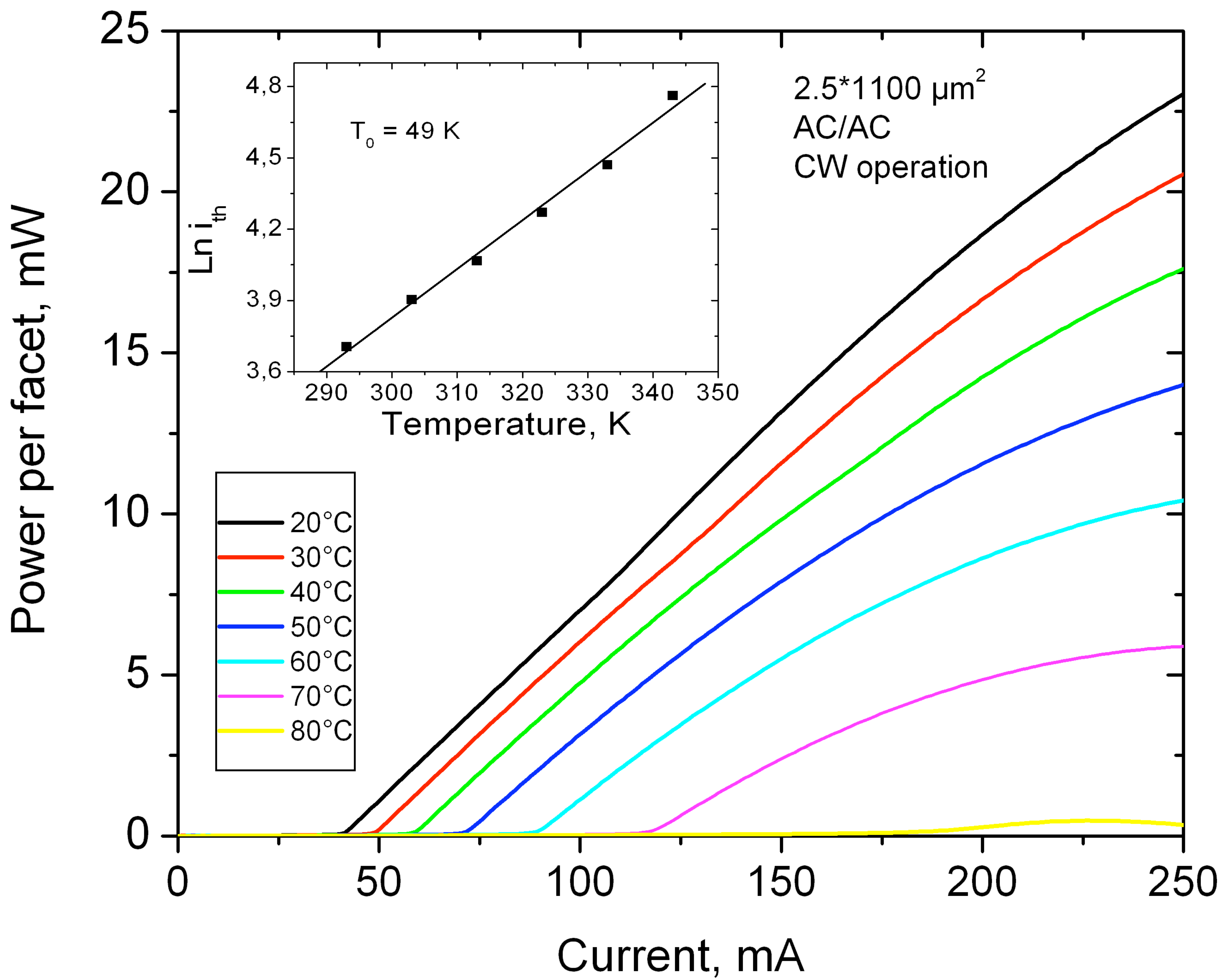

2.5*1100 μm2
AC/AC
CW operation
T0 = 49 K
Ln ith
Temperature, K
20°C
30°C
40°C
50°C
60°C
70°C
80°C
Power per facet, mW
Current, mA

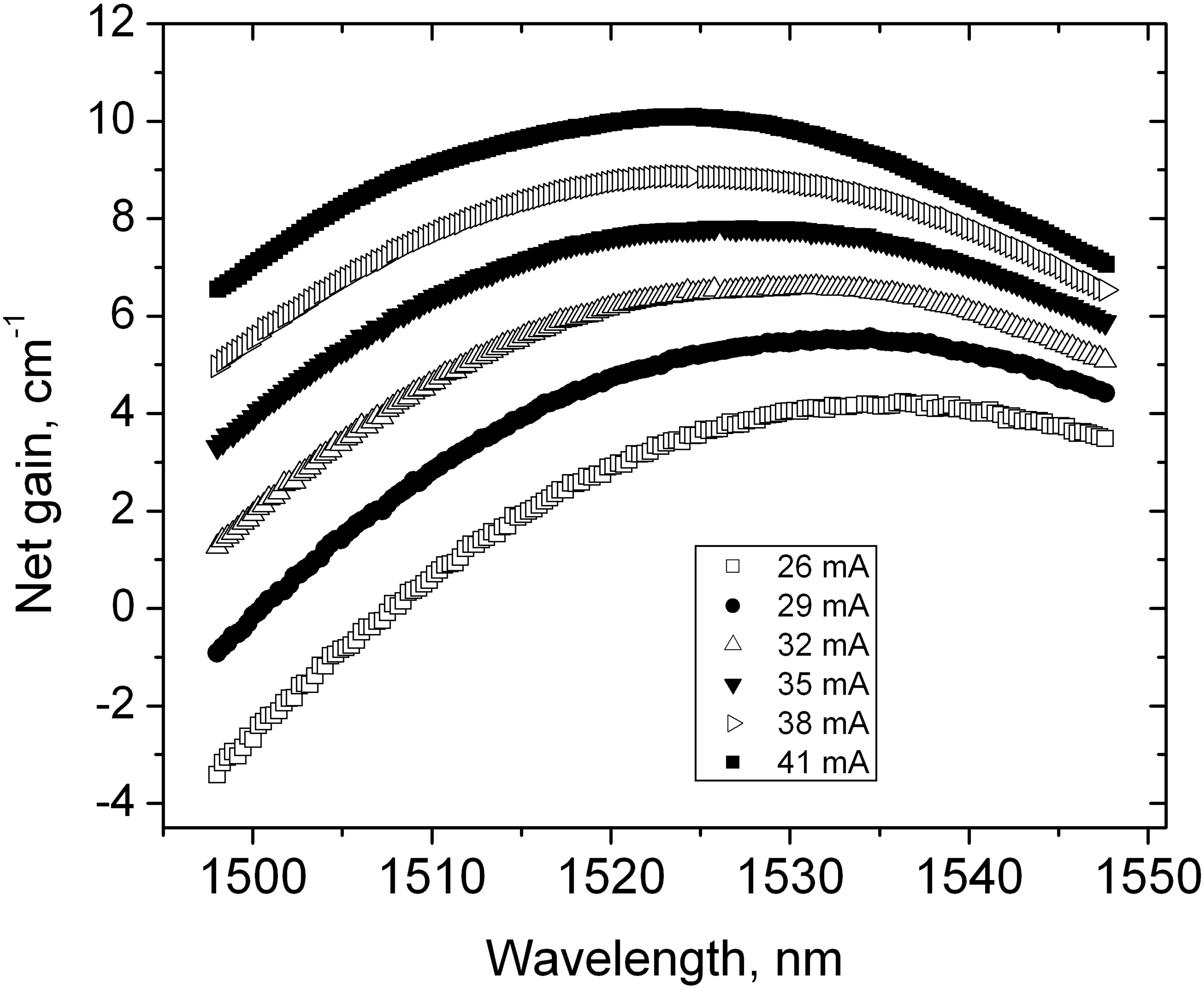

Net gain, cm^{-1}
Wavelength, nm
12
10
8
6
4
2
0
-2
-4
1500
1510
1520
1530
1540
1550
26 mA
29 mA
32 mA
35 mA
38 mA
41 mA

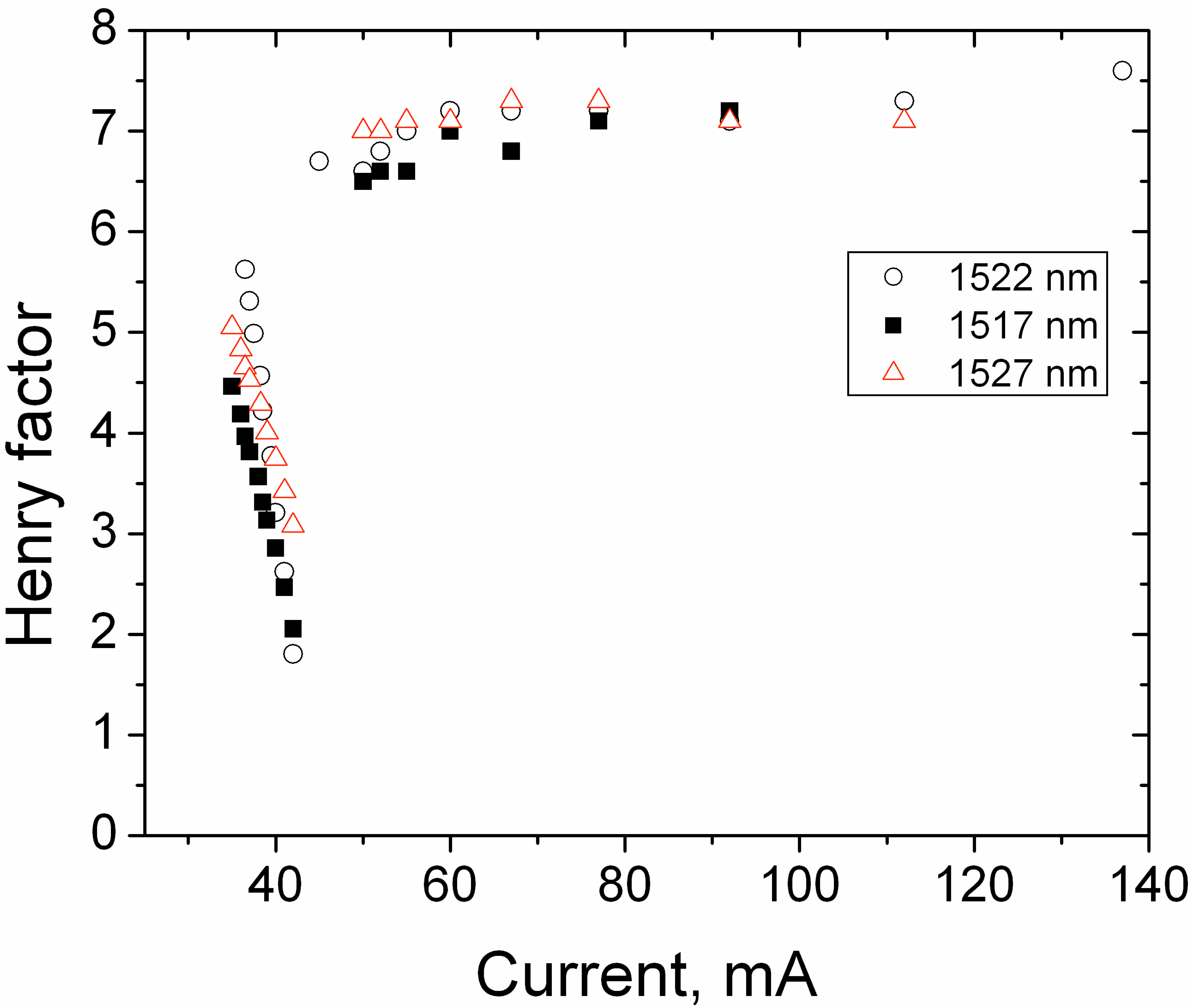

Henry factor
Current, mA
0
1
2
3
4
5
6
7
8
40
60
80
100
120
140
1522 nm
1517 nm
1527 nm

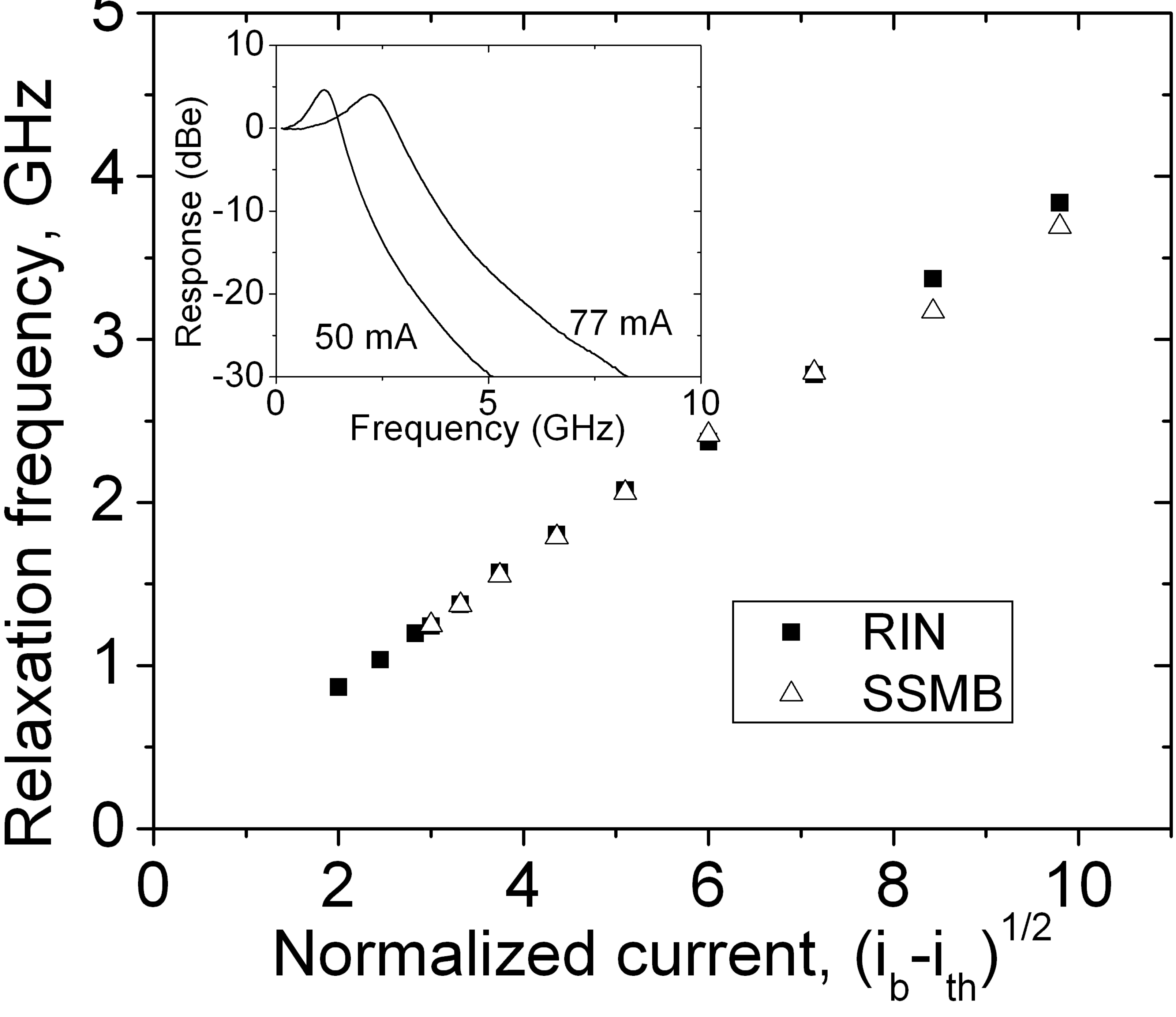

Relaxation frequency, GHz
Normalized current, $(i_b-i_{th})^{1/2}$
0
1
2
3
4
5
0
2
4
6
8
10
RIN
SSMB
Response (dBe)
Frequency (GHz)
10
0
-10
-20
-30
0
5
10
50 mA
77 mA